Fluid and Petrophysical Prediction in the Elastic Impedance Domain Using Neural Network Technique*

M. Hermana[1], M. Najmi[1], Z.Z.T. Harith[1], and C.W. Sum[1]

Search and Discovery Article #41066 (2012)*
Posted November 19, 2012

*Adapted from extended abstract prepared in conjunction with oral presentation at AAPG International Convention and Exhibition, Singapore, 16-19 September 2012, AAPG©2012

[1]Universiti Teknologi Petronas, Tronoh, Malaysia (mherjody@yahoo.com)

Abstract

Interpretation in elastic impedance domain is a new method in geophysical prospect evaluation and development. Inspired by the success in lithology and fluid discrimination in elastic domain, we applied Neural Network technique into elastic volume to predict fluid and petrophysical properties in the reservoir. The study consists of four phases: 1) Correlation study between elastic impedance log and petrophysical log to determine the optimum chi angle; 2) Construction of seismic equivalent from AVO attribute and Extended Elastic Impedance (EEI) projection; 3) inversion of EEI reflectivity into impedance domain using deterministic inversion technique; and 4) supervised ANN method used to determined fluid and petrophysical properties. The result showing that application of ANN can improve the correlation between log properties and EEI-petrophysical properties, which is derived from seismic.

Introduction

Inversion of seismic data into Acoustic Impedance (AI) including various inversion techniques is common workflow for reservoir characterization. Unfortunately, in some cases such as in low AI contrast, sand is difficult to be distinguished from shale such as at the field with argillite enriched. Hence, there is a need to find out an alternative method to full fill this limitation from seismic method for better reservoir characterization.

Interpretation based on elastic impedance, rather than AI, would be an alternative method to answer this difficulty. In this paper, the seismic volume of well log properties such as gamma ray (GR) will be derived to characterize reservoirs in terms of elastic impedance angle dependent. Supervised Artificial Neural Network (ANN) will be used on this seismic elastic impedance volume to improve correlation with wells.

Extended Elastic Impedance (EEI) technique is a new method in seismic exploration and has been applied in some fields. Whitcombe et al. (2002) estimate the water saturation and gamma ray logs from EEI using data from the Forties field in the central North Sea. Neves et al. (2004) estimate gamma ray logs for a gas play in central Saudi Arabia. Both sets of authors calculate the correlation coefficients between appropriate petrophysical log with the EEI logs between -90° and +90°. The correlations coefficient indicate how well a given petrophysics log can be predicted from seismic data, how an EEI log should be rotated, and how independently the petrophysics logs can be estimated. Success of this technique for reservoir characterization also has been reported by Arsalan and Yadav (2009) at Krishna-Godavari Basin, India.

Application of Neural Network technology for oil and gas exploration has been carried out widely. Wong et.al. (1995) used Neural Network for better porosity prediction. Mohaghegh et.al. (2004) used fuzzy logic and neural networks for determining the in-situ stress profile of hydrocarbon reservoirs.

In this study, neural network will be used to predict physical properties of reservoir based on elastic impedance. Volume of Gamma ray and water saturation volume equivalent is used for lithology and fluid prediction.

Basics of Extended Elastic Impedance

Extended Elastic Impedance was introduced to improve the limitation on Elastic Impedance theory for rock properties prediction. In the Elastic Impedance theory, some properties of rock cannot be predicted from existing seismic gathering due to limitations on incidence angles. Hence, the EEI concept was introduced to extend the angle from 0-30 degrees to -90 to 90 degrees in theory (Hicks et al., 2006). Consequently, the rock properties that associate with higher angles can be predicted.

Elastic Impedance (EI) is the other form of projection of 2-term AVO linearization; the $\sin^2\theta$ term was replaced by $\tan\chi$ (Hicks et al., 2006). This angle range is more powerful to accommodate more petrophysical properties that correlated with higher angles.

Concept of EEI can be derived from 2-term AVO equation as follows (Hicks et al., 2006).

$$R(\theta) = A + B \sin^2\theta \qquad (1)$$

where A and B are the intercept and gradient in 2-term AVO. By changing $\sin^2\theta$ with $\tan\chi$, the equation would be:

$$R(\theta) = A + B \tan\chi \qquad (2)$$

Scaling this equation by $\cos \chi$, the scaled reflectivity can be obtained:

$$Rs(\theta) = A \cos \chi, + B \sin \chi \qquad (3)$$

When Rs goes to zero, the relationship between AVO attribute with rotation angle can be calculated:

$$\text{Tan } \chi = - A/B \qquad (4)$$

Hicks et al. (2006) and Verma and Sibwal (2011) refer to the angle χ as "minimum energy χ" at which the reflectivity is defined by the two-term AVO equation is zero. It is the angle that the trend line in an AVO cross plot subtends to the negative B axis.

The equivalent expression for equation (3) as EEI is:

$$EEI(\chi) = \alpha_o \rho_o \left[\left(\frac{\alpha}{\alpha_o}\right)^p \left(\frac{\beta}{\beta_o}\right)^q \left(\frac{\rho}{\rho_o}\right)^r \right] \tag{5}$$

where α = P-wave velocity, ρ = density, β = S-wave velocity, $p = \cos\chi + \sin\chi$, $q = -8K \sin\chi$, and $r = \cos\chi - 4K \sin\chi$. $\alpha 0$, $\beta 0$, and $\rho 0$ are the average of the respective property used as normalization factors for P velocity, S velocity, and density, respectively. K is the average of $(V_S/V_P)^2$.

Available Data and Methods

In this study, we apply the flow work on Penobscot, Scotia Basin, Nova Scotia Department of Energy Canada. This data are available at the Opendtect Seismic repository site. The data consist of seismic data, wells and interpretations of horizons. Some of the petrophysical logs of Penobscot are shown in the Figure 1.

Petrophysical properties are estimated from seismic parameters based on EEI correlation, the optimum chi angle is then used for estimating petrophysical volumes from seismic data. EEI logs are generated from velocity and density log using equation (5), meanwhile the S-wave velocity log is estimated using Greenberg Castagna's equation.

For lithological prediction, the EEI-Gamma ray log correlation was performed to determine the optimum chi angle for lithological prediction. In this field, correlation between gamma ray logs with EEI occurs at 34 degrees. Meanwhile, the fluid prediction is performed based on correlation between EEI logs with water saturation logs. The chi angle for this correlation is 24 degrees.

The AVO attribute (Intercept and Gradient) was derived from pre-stack data based on two terms AVO equation. This intercept and gradient was used to construct seismic volume of rock properties equivalent through projection into certain chi angle using equation (3). Wavelet for appropriate seismic equivalent was generated using statistical method for appropriate well log and seismic volume. This wavelet is used to invert reflectivity volume into elastic volume using deterministic inversion. Finally, Neural Network is applied into EEI volume to improve the interpretation and well-seismic correlation. Summary of this flow is represented on Figure 2.

Results and Discussion

Correlation between EEI logs with petrophysical logs show that gamma ray logs have significant correlation with EEI at 34 degrees with the coefficient correlation is about 0.6. Meanwhile the EEI-water saturation logs correlation show that the maximum correlation occurs at 24-25 degrees with maximum coefficient correlation is 0.78. The angle and its coefficient correlation between EEI with other logs are shown in

Figure 3b. This angle is used for AVO rotation to construct seismic volume equivalent. Comparisons between EEI logs with appropriate petrophysical logs are shown in the Figure 3a.

From Figure 3 we can see that correlation between EEI logs with petrophysical logs are quite good, hence, the petrophysical prediction from seismic data can be performed. The trend of the well is relatively worthy represented by EEI logs. Unfortunately, in the high frequency, the high spike especially on the water saturation log is not represented by EEI log. However, this high frequency is not to be presented on seismic data until the resolution of seismic data is improved.

Supervised ANN method is implemented on seismic volume of GR and water saturation equivalent after deterministic inversion. Two logs of Penobscot well, gamma ray log and water saturation log, are used separately for training. During the training phase, 30% of well data was used. The training was stopped when normalized errors are at a minimum as shown in the Figure 4.

Relation between gamma ray log and gamma ray equivalent that was generated from EEI was improved through application of ANN on the elastic impedance domain. Comparison relation between both of them before and after ANN is shown in the Figure 5.

Slicing seismic data at Logan Canyon Formation shows that sand can be delineated clearly as shown in the Figure 6. In vertical view, the gamma ray log is plotted on EEI cross section data. It is clear that the seismic volume of EEI represents the lithology as also shown in Figure 6 (right). Different lamination on EEI data is fitting with the gamma ray log.

Light oil or condensate was discovered in early Cretaceous sandstones and Jurassic sandstones and carbonates in the following formations: Wyandot, Dawson Canyon, Logan Canyon, O marker, and Mississauga. The lower Logan Canyon sands in L-30 were considered oil bearing. Slicing at Pay Sand-2 formation from water saturation volume shows the possibility of gas/oil-water contact is clearly delineated (Figure 7).

Conclusion

Extended Elastic Impedance (EEI) can potentially be used for fluid and lithological prediction by doing some correlation and projection into certain chi angles. Application of ANN on the elastic impedance domain can improve the relationship between seismic equivalents and well logs.

References

Arsalan, S.I., and A. Yadav, 2009, Application of extended elastic impedance: A case study from Krishna-Godavari Basin, India: The Leading Edge, v. 28/10, p. 1204-1209.

Hicks, G.J., and A.M. Francis, 2006, Extended Elastic Impedance and Its Relation to AVO Crossplotting and Vp/Vs: EAGE 68th Conference & Technical Exhibition, v. 67, Abstract 496.

Mohaghegh, S.D., A. Popa, R. Gaskari, S. Wolhart, R. Siegfreid, and S. Ameri, 2004, Determining In-Situ Stress Profiles From Logs: SPE 90070, 6 p. Web accessed 6 November 2012.

Neves, F.A., H.M. Mustafa, and P.M. Rutty, 2004, Pseudo-gamma ray volume from Extended Elastic Impedance inversion for gas exploration: The Leading Edge, v. 23/6, p. 536-540.

Verma, S., and S. Biswal, 2011. Estimation of Effective Porosity and saturation volume by Extended Elastic Impedance approach : A case study: Search and Discovery Article #90118. Web accessed 6 November 2012. http://www.searchanddiscovery.com/abstracts/pdf/2011/geo-india/abstracts/ndx_verma.pdf

Whitcombe, D.N., P.A. Connolly, R.L. Reagan, and T.C. Redshaw, 2002, Extended elastic impedance for fluid and lithology prediction: Geophysics, v. 67/1, p. 63-67.

Wong, P.M., D. Gedeon, and I.J. Taggart, 1995, An Improved Technique in Porosity Prediction : A Neural Network Approach: IEEE Transactions on Geoscience and Remote Sensing, v. 33/4, p. 971-980.

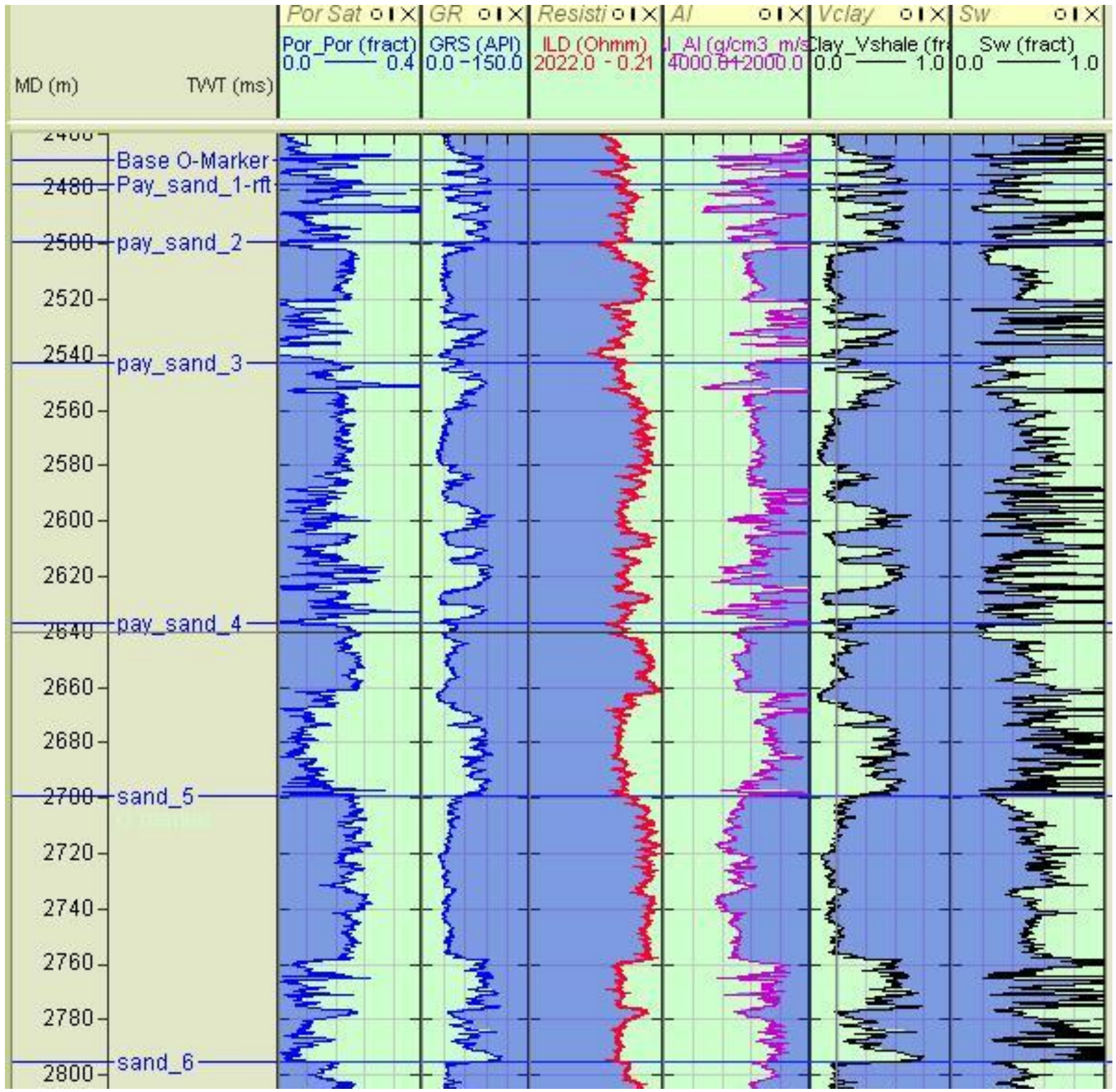

Figure 1. Well log of Penobscot Field. The porosity, gamma ray, resistivity, acoustic impedance, clay volume and water saturation log respectively.

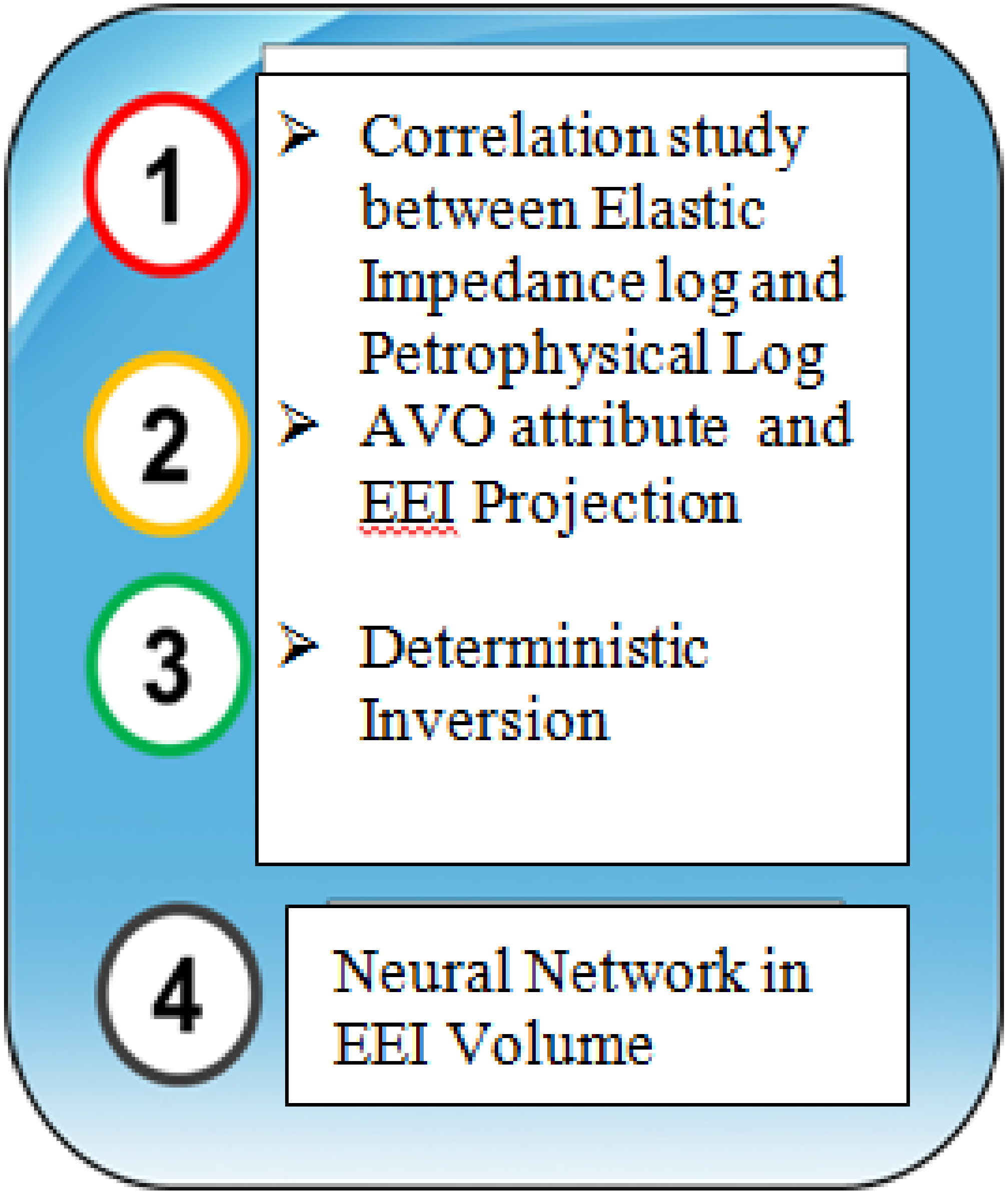

Figure 2. Flowchart of fluid and lithology prediction in Elastic Impedance Domain.

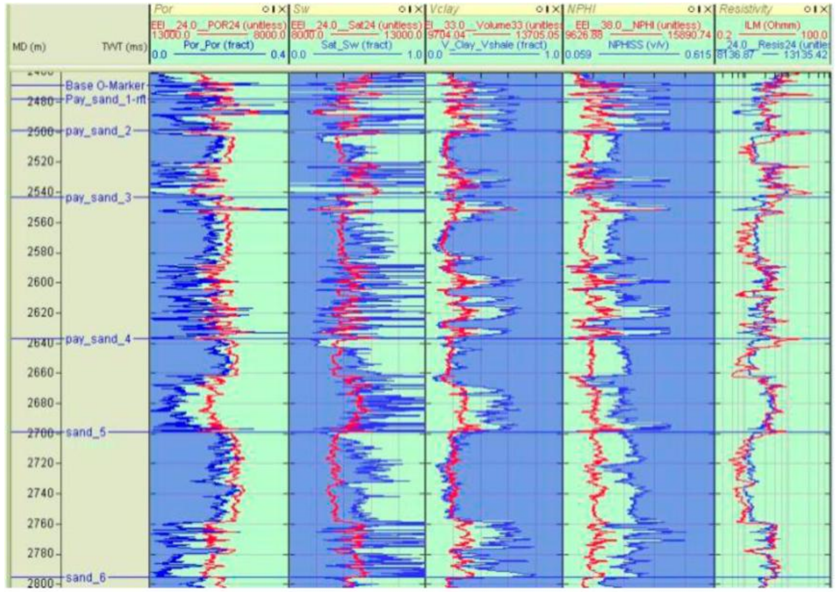

(a)

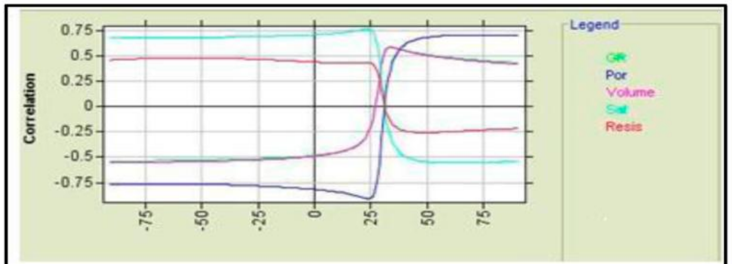

Parameter	χ(°)	Coef.Corr
Pore	24.15	-0.923
Volume	33.21	0.59
Resistivity	24.78	0.43
Saturation	24.76	0.78
GR	33.8	0.59

(b)

Figure 3. Comparison between log properties (blue line) and EEI log (red line) for appropriate petrophysical logs: porosity, water saturation, volume of clay, neutron and lateral logs (a) and its coefficient correlation curve (b).

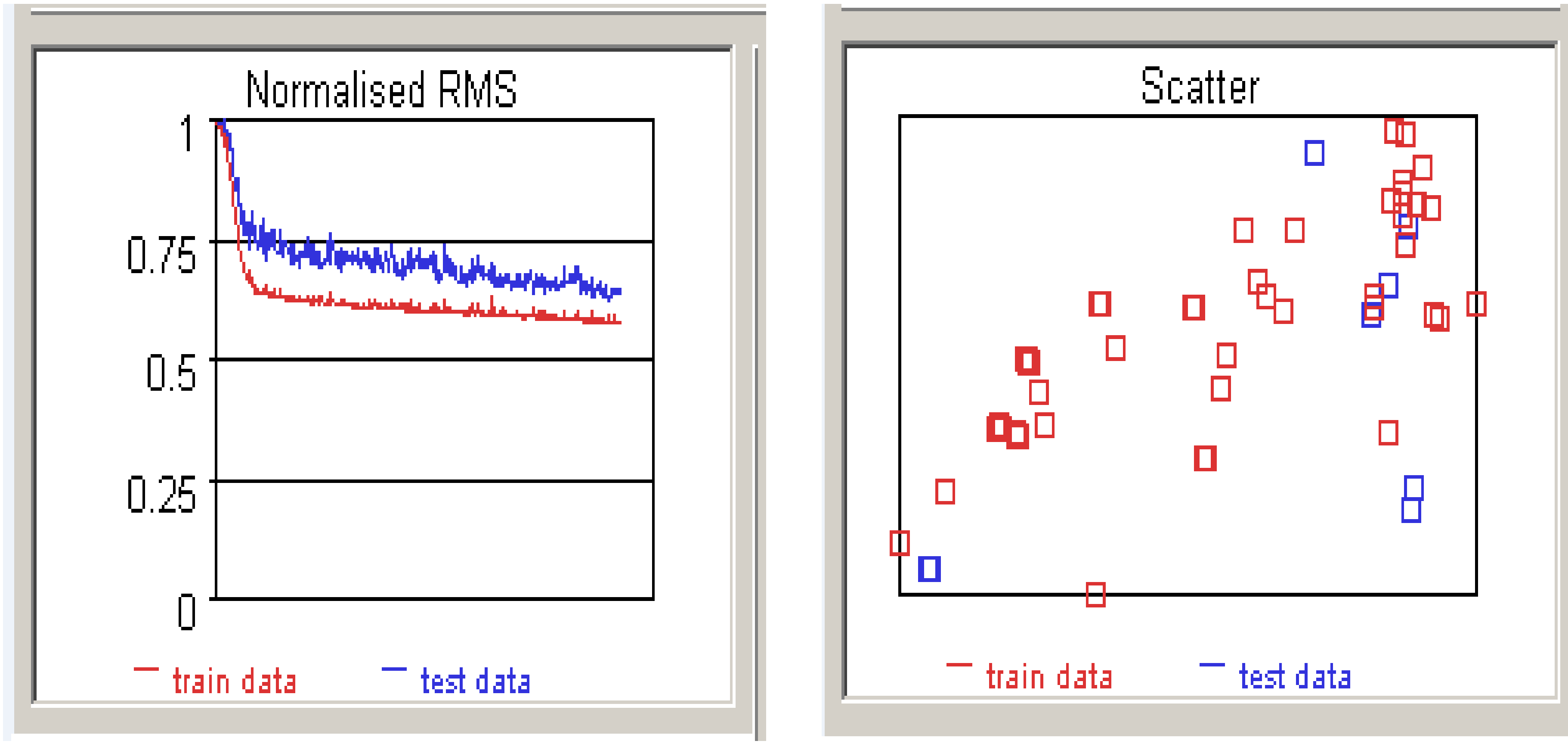

Figure 4. Normalized Errors between train data and test data (left) and plot scattering of train data and test data (right).

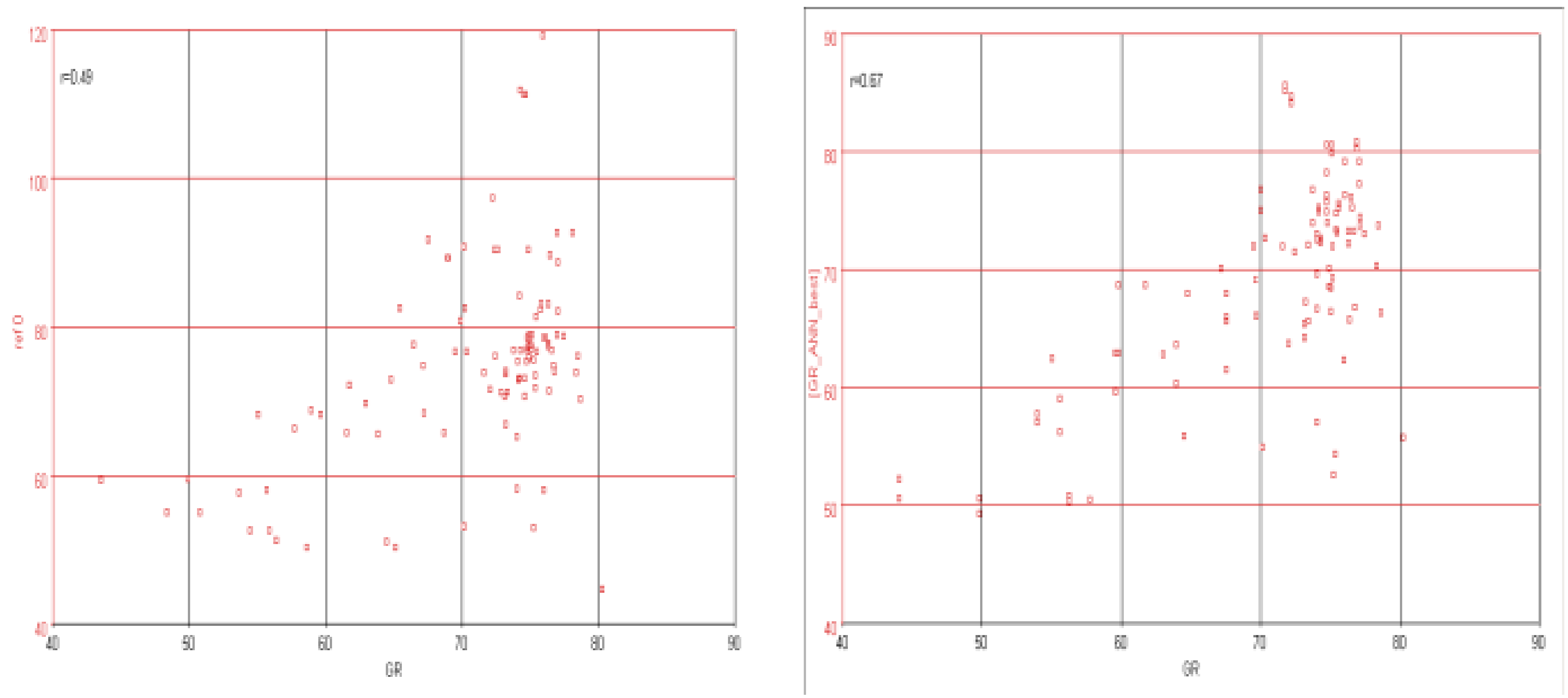

Figure 5. Crossplot between log gamma ray and gamma ray equivalent are extracted from seismic before (left) and after (right) ANN.

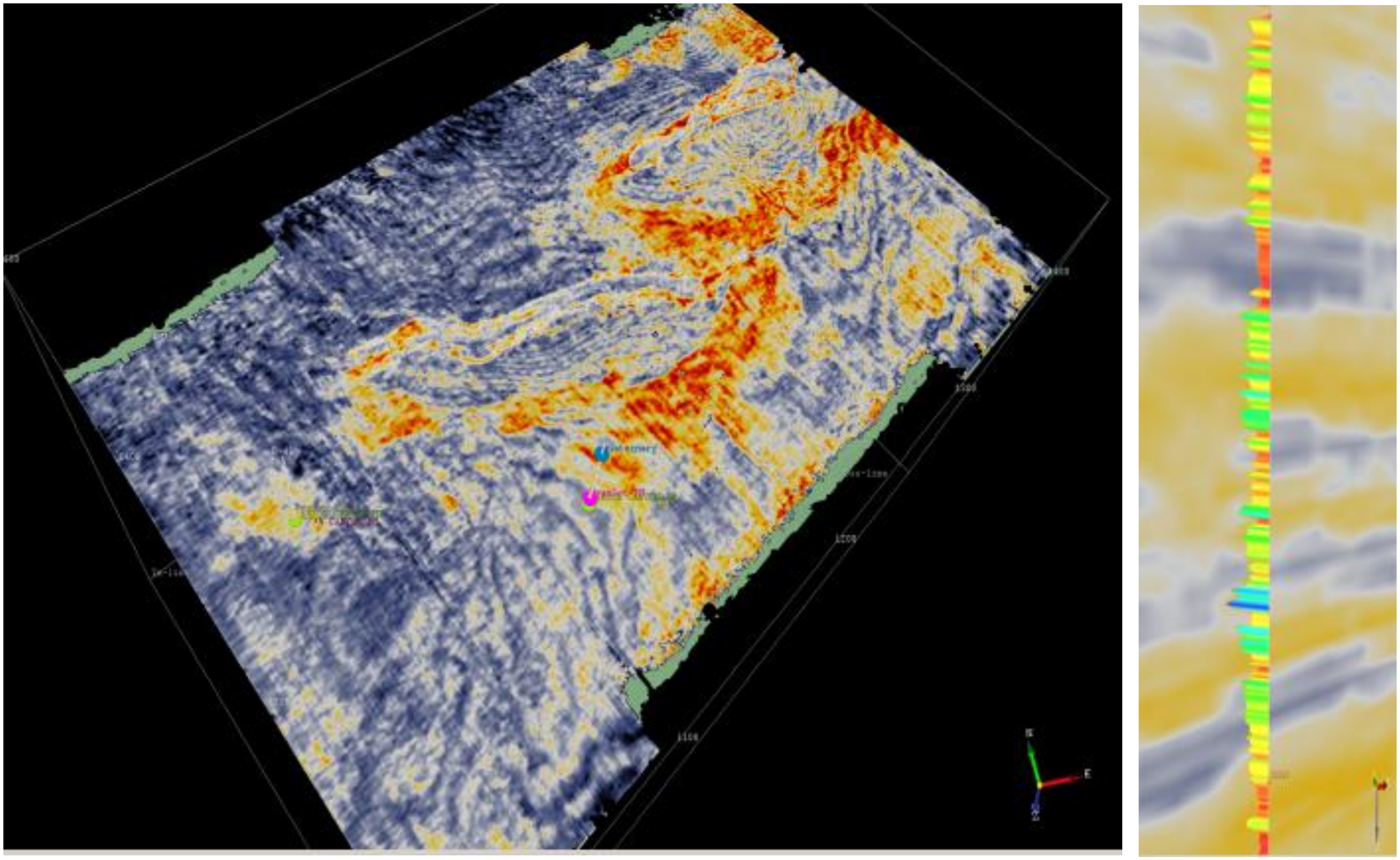

Figure 6. Slicing of gamma ray volume at Logan Canyon Formation (left) and cross section of gamma ray volume with gamma ray log.

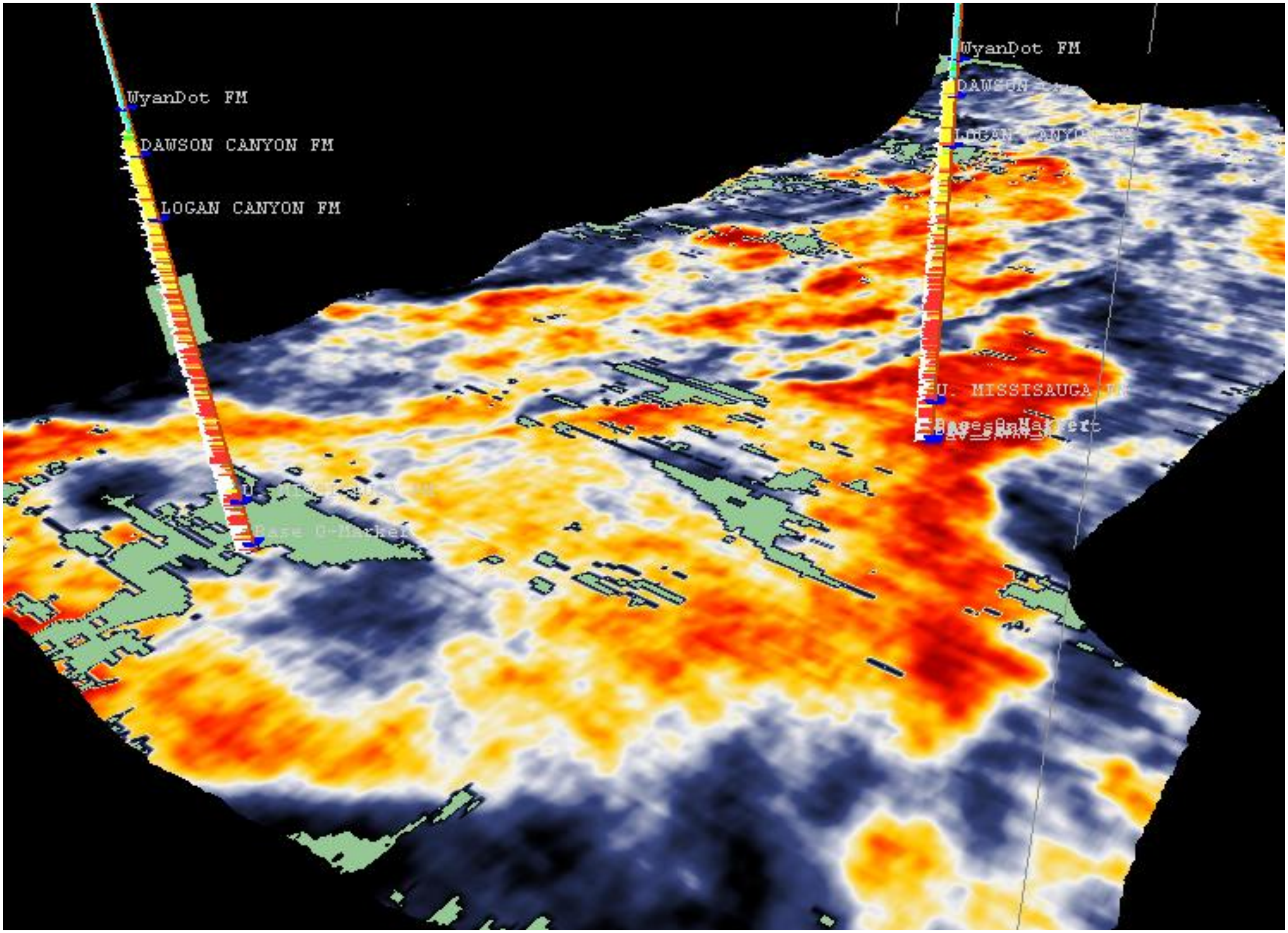

Figure 7. Slicing of water saturation volume generated from EEI (24) at Pay Sand-2 formation.